Sustainable Energy & Fuels

ROYAL SOCIETY OF CHEMISTRY

COMMUNICATION

View Article Online
View Journal | View Issue

Cite this: *Sustainable Energy Fuels*, 2022, **6**, 4388

Received 15th August 2022
Accepted 25th August 2022

DOI: 10.1039/d2se01119k

rsc.li/sustainable-energy

Simultaneous non-invasive gas analysis in artificial photosynthesis reactions using rotational Raman spectroscopy†

Jesper Schwarz, ‡[a] Aleksandra Ilic, ‡[a] Simon Kaufhold, [a] Jussi Ahokas, [b] Pasi Myllyperkiö, [b] Mika Pettersson [b] and Kenneth Wärnmark *[a]

Optimising reactions in artificial photosynthesis research requires screening of many reaction and operation parameters, which is often resource-intense and time-consuming. In this paper, we demonstrate the use of a rotational Raman-based spectrometer for non-invasive quantification of several gases (H_2, O_2, N_2, CO, CO_2) with short analysis times (15 s), enabling high throughput screening. Furthermore, with this device, reaction progress can be monitored *in situ*, by real-time simultaneous quantification of multiple gases. We have applied this instrument and developed a method to study the O_2 dependency of a prototypic light-driven hydrogen evolution reaction, showcasing the value of this approach for the artificial photosynthesis community in general.

The sustainable transformation of our society necessitates the shift from fossil resources to renewable feedstocks. Electrification, as well as a H_2- and circular carbon economy, will play a pivotal part in this process. Inspired by nature, researchers in chemical, biological and materials sciences have set out to contribute to this transformation by investigating artificial photosynthesis (AP) approaches.[1–3] AP aims to produce high-energy chemicals like H_2 (and O_2) or *e.g.* CO, formate or methanol, from abundant resources like H_2O, CO_2 and light. However, extensive screening for ideal reaction/operation conditions is often necessary due to the complexity of many AP systems. Additionally, synthesis or preparation of the (light-driven) catalysts or the phototropic microorganisms/enzymes is often laborious and resource-intense. Therefore, ways of carrying out these optimisation reactions on a small scale so as to minimise sample consumption are highly sought-after.

Common methods for gas analysis used in AP research labs include (micro) gas chromatography (GC),[4] mass spectrometry (MS),[5] (Clark-type) electrode sensors[6,7] or optical O_2 sensors.[8] While some of these methods have high sensitivity (ppm range) and fast measurement times (μs–ms), apart from optical sensors,[8] they usually require penetration of the reaction vessel to remove a sample volume or bring the sensor into contact with the sample. This holds the risk of leakage and/or contamination of the reaction medium or even consumption of non-negligible amounts of the gas sample, which in turn interferes with fast and reliable analysis and reaction screening. From our observation, Clark-type electrode sensors can face stability issues in reaction media containing organic solvents and additives like amines, thus potentially giving incorrect values. Similarly, for GC in AP, trapping columns are often needed to avoid deterioration of the GC column.

To overcome these constraints, we investigated the use of a device based on rotational Raman spectroscopy for the non-invasive analysis of H_2, O_2 and N_2, and potentially CO and CO_2, with 1% relative standard deviation (RSD) at 10s of seconds measurement times. Specifically, we looked at the simultaneous analysis of H_2 and O_2 in a known light-driven hydrogen evolution reaction (HER) system to exemplify the utility for developing AP systems. Raman spectroscopy of gases[9,10] has in recent years been improved through the use of Fibre Enhanced Raman Spectroscopy (FERS)[11] and Cavity Enhanced Raman Spectroscopy (CERS).[12] These techniques increase the pathlength of the light, thus increasing the signal strength, which has enabled the analysis of gases such as H_2 and hydrocarbons down to ppm levels.[13] However, the drawback of these systems is also that they require physical sampling of the gaseous analyte. In comparison to absorption-based techniques for gas analysis, such as IR, Raman spectroscopy is still far less common, because the signal strength is orders of magnitudes lower. A distinct advantage of Raman spectroscopy over IR spectroscopy is that IR inactive molecules such as nitrogen can be detected.

[a]*Centre for Analysis and Synthesis (CAS), Department of Chemistry, Lund University, SE-22100 Lund, Sweden. E-mail: kenneth.wärnmark@chem.lu.se*

[b]*Department of Chemistry, Nanoscience Center, University of Jyväskylä, FI-40014, Finland*

† Electronic supplementary information (ESI) available. See https://doi.org/10.1039/d2se01119k

‡ These authors contributed equally.

A new Raman gas analyser, developed by us, utilises the back-scattering geometry and rotational Raman spectrum of gaseous molecules.[14] This geometry enables a simple optical layout where a single lens focuses the incident light to the sample and collects the Raman scattering (Fig. 1). In this way, gases in an optically transparent, closed container – *e.g.* glass vials – can be analysed non-invasively. Laser light travels from a source (CNI Laser MLL-U-532-200-3) to a primary optical path with mirrors and an edge filter (Semrock 532 nm RazorEdge® ultra-steep). The primary optical path goes through the midpoint of the edge filter. The edge filter reflects the laser light to the lens (focal length 50 mm). The lens focuses the light on a sample and then collects the Raman scattering from the sample before collimating it along the primary optical path. The Stokes part of the Raman scattering passes through the edge filter. The second edge filter is placed perpendicularly to the primary optical axis to filter out the remaining laser light from the Raman scattering. Then the scattered light is focused on the slit (~100–200 μm) with a lens (focal length 175 mm). A lens (focal length 350 mm) collimates the signal before the volume-phase holographic transmission grating (Wasatch Photonics, 2800 L mm^{-1}). After dispersing the signal, a lens (focal length 350 mm) focuses the signal on a CCD array (Andor iDus 401, 1024 × 127 pixel). The signal is collected with a custom-made software and analysed using library spectra of pure gases and a multicomponent optimisation procedure. The rotational Raman spectrum is rich in information, and many gases of interest in AP research (H_2, O_2, N_2, CO, CO_2) possess a rotational spectrum in a narrow spectral range that allows tailoring of a high sensitivity and high-resolution spectrometer in a fixed geometry. The spectra for O_2 and H_2 are completely separated, which is not a requisite, but is highly advantageous as it facilitates simultaneous measurement of both gases (Fig. 2).

The analysis of the collected spectrum is based on solving weight factors for the predefined calibration spectra, *i.e.* solving a set of simultaneous linear equations. In practice, there is also a need for a correction of broad luminescence from the sample vials (low order polynomial), scattering from the air in the light-path inside the instrument, and laser power and wavelength changes during long experiments or between the calibration and sample measurements (linear scaling factors resolved from the internal calibration signal). Those corrections are implemented in the analysis routine. This method allows for simultaneous and precise analysis of gases having strongly overlapping rotational Raman spectra, like for O_2, N_2, CO and CO_2, but also spectrally separated species like H_2. The device can analyse gas mixtures where constituents' gas contents vary between 0.5% and 100%. The lower limit is dependent on gas components and experimental conditions. For calibration of the instrument, an argon-filled glass vial (0-point) and a vial filled with the analyte gas (100%-point) were used.

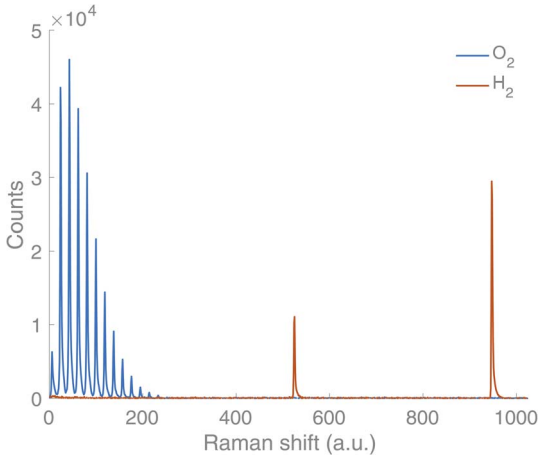

Fig. 2 Spectral signature of O_2 (blue) and H_2 (orange) from the Raman gas analyser.

Here, we demonstrate the use of this rotational Raman-based spectrometer for the non-invasive simultaneous real-time monitoring of H_2 and O_2. The system can quantify gases in small volumes, with each measurement taking 15 s, which enables high throughput screening of many reaction parameters. In order to establish the reliability of the instrument, we recorded calibration curves for H_2 and O_2. The data for the calibration curves were recorded by flushing a 4.9 mL glass vial with argon (which is Raman silent), followed by the addition of a known quantity of the gas analyte using a gas-tight syringe (Hamilton). The calibration curves showed excellent precision for H_2, with $R^2 > 0.999$ for concentrations in the range 40–5000

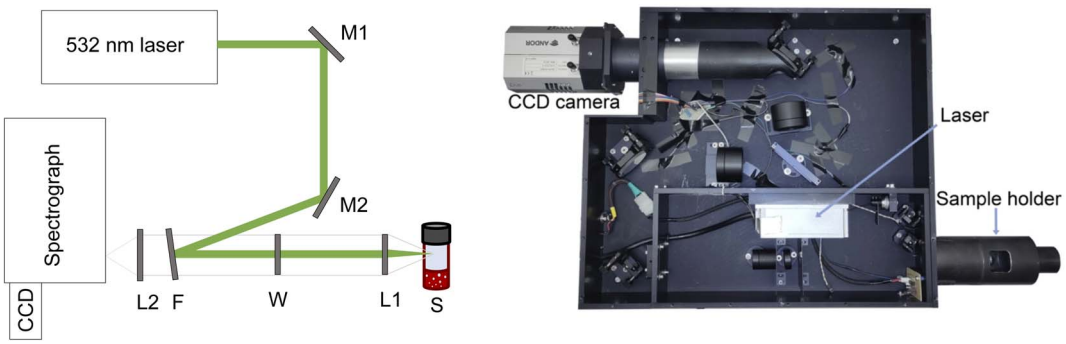

Fig. 1 Left: technical drawing of the Raman-based gas analyser. M = mirror, L = lens, F = edge filter, W = CaF_2 window, S = sample. Right: photo from above of the Raman gas analyser with the top cover removed.

μM H_2 in Ar, and $R^2 = 0.998$ up to 35 000 μM (Fig. S1–S4†). Furthermore, the accuracy of the instrument was evaluated against reference measurements using conventional Clark-type electrodes (Unisense). This showed that measurements were accurate within 3.5% relative to the Clark-type electrodes. The O_2 calibration curves coincided equally well with the Clark-type electrodes (0–8000 μmol L^{-1}, $R^2 = 0.9994$, Fig. S5†). In addition to H_2 and O_2, N_2, CO and CO_2 can be measured (Fig. S8–S10†). Quantification of CO and CO_2 is of particular interest in CO_2-reduction reactions. Although the spectra of these two gases partially overlap, they are sufficiently different so that they can be simultaneously reliably analysed (Fig. S11†). The distance between the spectral lines, as well as the intensities, are different for each gas.[15] We have recorded a calibration curve of different concentrations of CO in CO_2 (0–6000 μmol L^{-1}, $R^2 = 0.9985$, Fig. S6†) demonstrating that this instrument is potentially applicable to other AP reactions than HERs. In the same manner, O_2 and N_2 can be separated (Fig. S7†).

We then went on to study a conventional light-driven HER to gain further insight into the progression of the reaction and to test the system in a realistic setting. As a model HER, we chose the high turnover three component system developed by Leung *et al.*[16] The system consists of the photosensitiser (PS) $[Ir^{III}(dF(CF_3)ppy)_2(dtbbpy)]PF_6$ (0.03 mM),[17] the proton reduction catalyst (PRC) $[Co^{II}(qpy)(OH_2)_2](ClO_4)$ (qpy = 2,2′ : 6′,2″ : 6″,2‴-quaterpyridine)[16] (0.6 mM), the sacrificial reductant triethanolamine (TEOA) (0.2 M) and water (5% v/v) in acetonitrile (2 mL). Before irradiation of the solution, it was purged with argon. The reactions were carried out in 4.9 mL glass vials with screw cap septum lids (silicone/PTFE) using LED irradiation ($\lambda = 375$ nm, 45 mW) from below the vials. We have also used blue and green LED irradiation ($\lambda = 450$ nm and $\lambda = 525$ nm), without seeing any influence on the measurements, indicating that light sources placed below the sample do not interfere with the gas analysis. Initial simultaneous measurement of the H_2 production by Clark-type electrodes and the Raman gas analyser showed coinciding curves for the H_2 content in the headspace (Fig. 3).

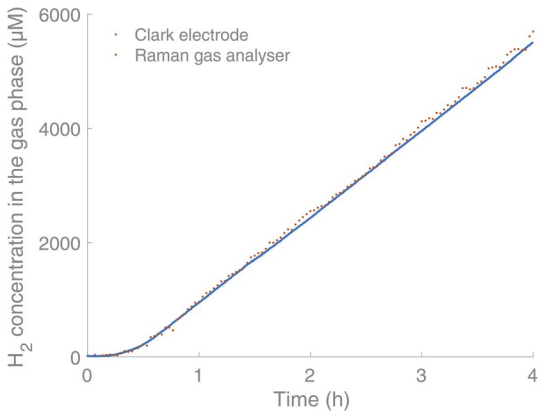

Fig. 3 Comparison between the Raman gas analyser (orange) and Clark electrodes (blue, Unisense) in real-time monitoring of H_2 in the headspace of a HER. Experimental conditions: $[Ir^{III}(dF(CF_3)ppy)_2(dtbbpy)]PF_6$ (0.03 mM),[17] $[Co^{II}(qpy)(OH_2)_2](ClO_4)$[16] (0.6 mM), TEOA (0.2 M) and water (5% v/v) in acetonitrile (2 mL).

Subsequently, we were interested in exploring the effect of O_2 on this HER. We were able to run the reaction and monitor the H_2 and O_2 content of the headspace in real-time during the irradiation period. In the absence of O_2, the H_2 formation started after an induction period of 40 minutes. We then proceeded on to add varying amounts of O_2, with a gas-tight syringe through the septum, before irradiation. When O_2 was added, we saw an initial consumption of O_2 before the H_2 formation started, and the induction period for H_2 formation was increased, from 2 h upon addition of 100 μL of O_2 and up to 4 h upon addition of 500 μL of O_2 (Fig. 4). H_2 formation started once the O_2 level fell below 300 μM in the gas phase, while the O_2 level continued decreasing down to near zero.

By fitting the O_2 concentration to a monoexponential decay, rate constants for the consumption of O_2 could be obtained. These showed similar rate constants independent of the initial concentration of O_2. For a starting concentration of 7600 μM of O_2 in the headspace (addition of 500 μL of O_2), the rate constant k was 1.84×10^{-4} s^{-1}. For a starting concentration of 3600 μM and 1900 μM of O_2 respectively, rate constants of $k = 2.54 \times 10^{-4}$ s^{-1} and $k = 2.00 \times 10^{-4}$ s^{-1} were obtained. The presence of O_2 together with a PS with a long-lived triplet exited state is known to induce the formation of reactive oxygen species like singlet oxygen through energy transfer.[18,19] Alternatively, the oxygen could be consumed through reduction to H_2O or H_2O_2.[20–22] The reactive oxygen species could, in turn, degrade the different components of the catalytic system. At the end of all the HERs performed using this system, with or without added O_2, a black suspension/precipitate formed, indicating a reduction of the cobalt catalyst to Co(0) and eventual particle formation. Small changes in this process could also explain the different rates of H_2 formation for the high O_2-concentration samples. As seen in Fig. 4, the gas analyser provides simultaneous real-time data of both the H_2 and O_2 concentrations in the headspace of the vial. For both gases, a few outliers can be observed in the curves. In longer measurements (>1000 datapoints) these usually occur a few times, due to cosmic rays hitting the CCD detector.[23] They can easily be omitted by fitting the data, but we have chosen to show the raw data including these artefacts for the sake of transparency. From this real-time monitoring of the two gases in parallel, we conclude that no H_2 formation is possible until the O_2 concentration has reached very low levels.

In addition to enabling the simultaneous quantification of gases, we found that efficient screening of reaction parameters is facile when using this instrument. This can primarily be attributed to two of its inherent advantages, as was shown in the recent development of an HER using an iron PS in combination with different proton reduction catalysts.[24] There, a measurement time of 25 s was used and three replicates were recorded, resulting in a total measurement time of less than 1.5 min per sample, while obtaining reliable data for each measurement (RSD = 1%). As a result of the short analysis time, the main factor limiting the number of reactions performed and tracked in parallel when choosing not to trace *in situ* is the irradiation set-up

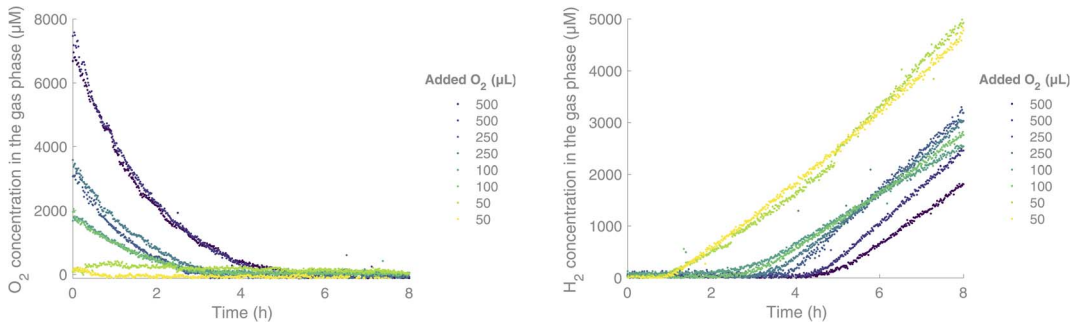

Fig. 4 Simultaneous measurement of O_2 (left) and H_2 (right) in a H_2 formation reaction, under Ar (g) with different added amounts of O_2 initially. Experimental conditions: $[Ir^{III}(dF(CF_3)ppy)_2(dtbbpy)]PF_6$ (0.03 mM),[17] $[Co^{II}(qpy)(OH_2)_2](ClO_4)$[16] (0.6 mM), TEOA (0.2 M) and water (5% v/v) in acetonitrile (2 mL).

itself, wherein only a certain number of reaction vials can be irradiated simultaneously, and not the analysis method. Furthermore, the non-invasive measurement by the gas analyser made repeated, continuous sample-taking from the same reaction possible without risking leakage induced by puncturing.

Additionally to being non-invasive, the quantification of the gas content using very small volumes of reaction solution (2 mL) in reaction vessels with a total volume of 4.9 mL (incl. headspace) is possible, both of which result in a highly economic way of optimising reaction conditions. The use of such a non-invasive set-up that allows for small-scale testing of reaction parameters thus leads to minimal wasting of precious materials (PSs, catalysts) in the search for ideal conditions. Finally, the comparably small reaction volumes also result in less organic solvent being required for the individual reactions, which is more cost-efficient and lowers the environmental impact of the optimisation.

In conclusion, we have demonstrated a rotational Raman-based spectrometer as a non-invasive method for real-time simultaneous analysis of gases in small volumes. While all Raman active gases (H_2, O_2, N_2, CO, CO_2) can be measured, we have particularly shown the O_2-concentration dependency of the onset of a common HER. This serves as one example of how this technique could considerably impact the future investigation and development of AP systems. We envision that this method will enable high throughput screening in AP, resulting in this very promising and impactful field advancing more rapidly. Additionally, the ability to analyse the composition of the gas phase in real time, combined with other *in situ* techniques, can hopefully provide deeper insight into the kinetics of AP reactions further facilitating optimisation of the studied systems.[25]

Conflicts of interest

There are no conflicts of interest to declare.

Acknowledgements

Jens Uhlig and Sarah Klingler are acknowledged for technical assistance and discussions. KW would like to thank the Swedish Foundation for Strategic Research (SSF, EM16-0067), the Knut and Alice Wallenberg Foundation (KAW, 2018.0074), the Swedish Research Council (VR, 2020-03207), the Swedish Energy Agency (Energimyndigheten), the LMK Foundation and the Sten K Johnson Foundation for financial support. SK acknowledges support from Wenner-Gren Stiftelserna and the Royal Physiographic Society of Lund.

References

1 S. Berardi, S. Drouet, L. Francàs, C. Gimbert-Suriñach, M. Guttentag, C. Richmond, T. Stoll and A. Llobet, *Chem. Soc. Rev.*, 2014, **43**, 7501.
2 E. S. Andreiadis, M. Chavarot-Kerlidou, M. Fontecave and V. Artero, *Photochem. Photobiol.*, 2011, **87**, 946.
3 B. Zhang and L. Sun, *Chem. Soc. Rev.*, 2019, **48**, 2216.
4 P. Du, J. Schneider, G. Luo, W. W. Brennessel and R. Eisenberg, *Inorg. Chem.*, 2009, **48**, 4952.
5 H. Park, H.-H. Ou, U. Kang, J. Choi and M. R. Hoffmann, *Catal. Today*, 2016, **266**, 153.
6 L. Li, L. Duan, F. Wen, C. Li, M. Wang, A. Hagfeldt and L. Sun, *Chem. Commun.*, 2012, **48**, 988.
7 A. C. Sander, S. Maji, L. Francàs, T. Böhnisch, S. Dechert, A. Llobet and F. Meyer, *ChemSusChem*, 2015, **8**, 1697.
8 F. L. Huber, S. Amthor, B. Schwarz, B. Mizaikoff, C. Streb and S. Rau, *Sustain. Energy Fuels*, 2018, **2**, 1974.
9 R. W. Wood, *Nature*, 1929, **123**, 279.
10 D. Schiel and W. Richter, *Fresenius' Z. Anal. Chem.*, 1987, **327**, 335.
11 A. Knebl, D. Yan, J. Popp and T. Frosch, *TrAC, Trends Anal. Chem.*, 2018, **103**, 230.
12 C. Niklas, H. Wackerbarth and G. Ctistis, *Sensors*, 2021, **21**, 1.
13 A. Knebl, C. Domes, R. Domes, S. Wolf, J. Popp and T. Frosch, *Anal. Chem.*, 2021, **93**, 10546.
14 J. Ahokas and M. Pettersson, WO 2013/079806 A1, 2013.
15 L. C. Hoskins, *J. Chem. Educ.*, 1975, **52**, 568.
16 C.-F. Leung, S.-M. Ng, C.-C. Ko, W.-L. Man, J. Wu, L. Chen and T.-C. Lau, *Energy Environ. Sci.*, 2012, **5**, 7903.
17 M. S. Lowry, J. I. Goldsmith, J. D. Slinker, R. Rohl, R. A. Pascal, G. G. Malliaras and S. Bernhard, *Chem. Mater.*, 2005, **17**, 5712.

18 T. Tachikawa and T. Majima, *Langmuir*, 2009, **25**, 7791.
19 B. Tian, W. Gao, X. Ning, Y. Wu and G. Lu, *Appl. Catal., B*, 2019, **249**, 138.
20 X. Guo, X. Li, X. C. Liu, P. Li, Z. Yao, J. Li, W. Zhang, J. P. Zhang, D. Xue and R. Cao, *Chem. Commun.*, 2018, **54**, 845.
21 C. Costentin, H. Dridi and J.-M. Savéant, *J. Am. Chem. Soc.*, 2015, **137**, 13535.
22 P. Yin, T. Yao, Y. Wu, L. Zheng, Y. Lin, W. Liu, H. Ju, J. Zhu, X. Hong, Z. Deng, G. Zhou, S. Wei and Y. Li, *Angew. Chem., Int. Ed.*, 2016, **55**, 10800.
23 D. Groom, *Exp. Astron.*, 2002, **14**, 45.
24 J. Schwarz, A. Ilic, C. Johnson, R. Lomoth and K. Wärnmark, *Chem. Commun.*, 2022, **58**, 5351.
25 S. Klingler, J. Hniopek, R. Stach, M. Schmitt, J. Popp and B. Mizaikoff, *ACS Meas. Sci. Au*, 2022, **2**, 157.